Quantum fluctuations of a resonantly interacting p-wave Fermi superfluid in two dimensions

Hui Hu,[1] Brendan C. Mulkerin,[1] Lianyi He,[2] Jia Wang,[1] and Xia-Ji Liu[1]

[1]*Centre for Quantum and Optical Science, Swinburne University of Technology, Melbourne, Victoria 3122, Australia*

[2]*Department of Physics and State Key Laboratory of Low-Dimensional Quantum Physics, Tsinghua University, Beijing 100084, China*

(Received 25 September 2018; published 4 December 2018)

Using the Gaussian pair fluctuation theory, we investigate quantum fluctuations of a strongly interacting two-dimensional chiral p-wave Fermi superfluid at the transition from a Bose-Einstein condensate (BEC) to a topologically nontrivial Bardeen-Cooper-Schrieffer superfluid. Near the topological phase transition at zero chemical potential, $\mu = 0$, we observe that quantum fluctuations strongly renormalize the zero-temperature equations of state, sound velocity, pair-breaking velocity, and Berezinskii-Kosterlitz-Thouless (BKT) critical temperature of the Fermi superfluid, all of which can be nonanalytic functions of the interaction strength. The indication of nonanalyticity is particularly evident in the BKT critical temperature, which also exhibits a pronounced peak near the topological phase transition. Across the transition and towards the BEC limit we find that the system quickly becomes a trivial interacting Bose liquid, whose properties are less dependent on the interparticle interaction. The qualitative behavior of composite bosons in the BEC limit remains to be understood.

DOI: 10.1103/PhysRevA.98.063605

I. INTRODUCTION

Unconventional electronic superconductivity and fermionic superfluidity are of great interest and lie at the heart of many intriguing quantum materials [1]. One of the most important examples is the two-dimensional (2D) chiral p-wave superconductor (superfluid), where the pairing order parameter has the $p_x + ip_y$ symmetry in its orbital angular momentum. It was shown to be topologically nontrivial with vortex excitations that exhibit non-Abelian statistics [2,3]. These so-called Majorana excitations have been suggested to be a key ingredient for processing topological quantum computation [4,5]. Unfortunately, in spite of extensive search for decades, a 2D p-wave superconductor remains elusive in condensed matter physics. The best-known candidate material of 2D p-wave superconductors so far is strontium ruthenate, Sr_2RuO_4, whose superconductivity was first observed by Maeno and his group in 1994 [6].

The recent realization of resonantly interacting ultracold atomic Fermi gases opens a new paradigm to create the topological p-wave superfluid [7]. By tuning the s-wave interparticle interaction in a two-component Fermi gas through magnetic Feshbach resonances, the crossover from a Bardeen-Cooper-Schrieffer (BCS) fermionic superfluid to a Bose-Einstein condensate (BEC) has now been routinely observed in laboratories [8,9], confirming the long-sought BEC-BCS crossover [10–13] in both three and two dimensions. A resonantly interacting p-wave Fermi gas can be realized by either using p-wave Feshbach resonances or by preparing fermionic atoms in the same hyperfine pseudospin state, which experience long-range dipole-dipole interactions. The former has already been demonstrated for ^{40}K and ^{6}Li atoms [14–25], although the system suffers a serious loss in atom number near the p-wave resonance. Nevertheless, in three dimensions the system can still reach a quasiequilibrium state [22], in which a number of interesting physical properties of the cloud can be experimentally examined. More importantly, in lower dimensions the atom loss has been found to be significantly reduced [23], as theoretically predicted [26,27]. For a single-component dipolar Fermi gas [28,29] the s-wave scattering is completely suppressed by the Pauli exclusion principle. The p-wave component of the interparticle interaction could then be significantly enhanced by suitably tuning the strength of the dipole-dipole interaction. All these recent experimental advances in ultracold atoms make the realization of a 2D p-wave Fermi superfluid a very appealing idea.

Theoretically, the many-body physics of strongly interacting p-wave Fermi gases has been studied to some extent [7]. These include the exploration of the phase diagram [30–35], which becomes richer due to the anisotropy in the different p-wave channels, determining the transition temperature for the superfluid transition in three dimensions [36–38] or the Berezinskii-Kosterlitz-Thouless (BKT) transition in two dimensions [39], as well as the calculation of the p-wave contact parameters [40–46], which characterize the universal short-distance and large-momentum behavior of the system [47,48]. Most of these theoretical investigations rely on the mean-field theory, which qualitatively captures the underlying physics of the p-wave pairing. To describe more accurately a p-wave Fermi superfluid, in particular in two dimensions, it is necessary to include strong quantum fluctuations beyond mean field close to the resonantly interacting regime [49,50]. In this respect, it is convenient to adopt the Gaussian pair fluctuation (GPF) theory [51,52], which provides a quantitatively reliable description of an s-wave Fermi superfluid at the BEC-BCS crossover, in both three [51–53] and two dimensions [54].

In this work, we explore quantum fluctuations in a 2D chiral p-wave Fermi superfluid using the GPF theory, paying specific attention to the role played by the topological phase transition at zero chemical potential. A number of

 ©2018 American Physical Society

physical observables at zero temperature are considered across the BEC-BCS transition, such as the chemical potential, total energy, pressure equation of state, sound velocity, pair-breaking velocity, and also the critical velocity for superfluidity. All these quantities are strongly affected by quantum fluctuations. By assuming the existence of well-defined fermionic Bogoliubov quasiparticles and bosonic excitations of phonons, we further calculate the temperature dependence of superfluid fraction with the approximate Landau formalism [55]. This leads to an improved determination of the BKT critical temperature in the strongly interacting regime.

The paper is organized as follows. In the next section (Sec. II), we present the model Hamiltonian of a 2D spinless p-wave interacting Fermi gas. In Sec. III, we describe the details of the GPF theory of the chiral p-wave Fermi superfluid. In Sec. IV, we first discuss various equations of state as a function of the interaction strength, including the chemical potential, pressure, and total energy. We then present the results of sound velocity, pair-breaking velocity, and critical velocity. Based on the single-particle fermionic excitation spectrum and the sound velocity at zero temperature, we calculate the temperature dependence of superfluid density within the Landau picture for superfluidity and consequently determine the BKT critical temperature. Finally, in Sec. V we give our conclusions and outlook.

II. MODEL HAMILTONIAN

We consider a spinless 2D atomic Fermi gas of density n, interacting in the dominant p-wave channel near a broad p-wave Feshbach resonance, as described by a single-channel Hamiltonian (we set the area $A = 1$) [30],

$$\mathcal{H} = \sum_{\mathbf{k}} \xi_{\mathbf{k}} \psi_{\mathbf{k}}^{\dagger} \psi_{\mathbf{k}} + \frac{1}{2} \sum_{\mathbf{k},\mathbf{k}',\mathbf{q}} V_{\mathbf{k}\mathbf{k}'} b_{\mathbf{k}\mathbf{q}}^{\dagger} b_{\mathbf{k}'\mathbf{q}}, \tag{1}$$

where $\psi_{\mathbf{k}}$ ($\psi_{\mathbf{k}}^{\dagger}$) is the annihilation (creation) field operator for atoms with mass M and the single-particle dispersion $\xi_{\mathbf{k}} \equiv \epsilon_{\mathbf{k}} - \mu = \hbar^2 \mathbf{k}^2/(2M) - \mu$, and $b_{\mathbf{k}\mathbf{q}} \equiv \psi_{-\mathbf{k}+\mathbf{q}/2} \psi_{\mathbf{k}+\mathbf{q}/2}$ is the composite operator that annihilates a pair of atoms with a center-of-mass momentum $\mathbf{q}$. We work with the grand-canonical ensemble and tune the chemical potential μ to make the average density

$$\sum_{\mathbf{k}} \langle \hat{n}_{\mathbf{k}} \rangle = n \equiv \frac{k_F^2}{4\pi}, \tag{2}$$

where $\hat{n}_{\mathbf{k}} \equiv \psi_{\mathbf{k}}^{\dagger} \psi_{\mathbf{k}}$ and k_F is the Fermi wave vector. For the interparticle interaction, we adopt the following separable form [12,30,31],

$$V_{\mathbf{k}\mathbf{k}'} = \lambda \Gamma(\mathbf{k}) \Gamma^*(\mathbf{k}'), \tag{3}$$

where $\lambda < 0$ is the *bare* interaction strength and the dimensionless regularization function $\Gamma(\mathbf{k})$ represents the chiral $p_x + ip_y$ symmetry of the pairing interaction, i.e.,

$$\Gamma(\mathbf{k}) = \frac{(k/k_F)}{[1 + (k/k_0)^{2n}]^{3/2}} e^{i\varphi_{\mathbf{k}}}. \tag{4}$$

Here, k_0 is a large momentum cutoff, which is necessary to make the model Hamiltonian renormalizable, and $\varphi_{\mathbf{k}}$ is the polar angle of $\mathbf{k}$. We use the exponent n to tune the shape of the regularization function $\Gamma(\mathbf{k})$ and to confirm the insensitivity of our results on the form of the interparticle interaction. The choice of $n = 1/2$ was used earlier by Noziéres and Schmitt-Rink [12], and Botelho and Sá de Melo [30]. In this paper, unless otherwise specified, we follow the work by Ho and Diener [31] and take $n = 1$ for the numerical results presented. Actually, the results depend very weakly on the exponent n. The use of other values of n only leads to small quantitative difference.

In principle, the bare interaction strength λ and the cutoff momentum k_0 should be renormalized (i.e., replaced) in terms of the 2D p-wave scattering area a_p and effective range $R_p \sim 1/k_0$ [44]. However, for a better presentation, it turns out to be more convenient to use a scattering energy E_b [30,39], which is basically the ground-state energy of two fermions at zero center-of-mass momentum,

$$2\epsilon_{\mathbf{k}} \psi_{\mathbf{k}} + \sum_{\mathbf{k}'} V_{\mathbf{k}\mathbf{k}'} \psi_{\mathbf{k}'} = E_b \psi_{\mathbf{k}}. \tag{5}$$

By inserting the separable interaction potential, it is easy to obtain

$$\frac{1}{\lambda} = -\sum_{\mathbf{k}} \frac{|\Gamma(\mathbf{k})|^2}{2\epsilon_{\mathbf{k}} - E_b}. \tag{6}$$

We note that, unlike the s-wave scattering in two dimensions, where the scattering energy E_b is always negative, in our p-wave case E_b can be either negative or positive. A negative scattering energy indicates the existence of a two-body bound state (i.e., on the BEC side), with a binding energy $\varepsilon_B = -E_b > 0$. On the other hand, the weakly interacting BCS limit is reached at $E_b \to +\infty$. Throughout the paper, we use the set of parameters $E_b, k_0, n = 1$ to characterize the p-wave interaction. Their relation to the p-wave scattering area a_p and effective range R_p is briefly discussed in Appendix A.

III. GAUSSIAN PAIR FUNCTION THEORY AT ZERO TEMPERATURE

In the superfluid phase at zero temperature, it is useful to introduce the Nambu spinor presentation for the field operators [51,52],

$$\Psi_{\mathbf{k}} = \begin{pmatrix} \psi_{\mathbf{k}} \\ \psi_{-\mathbf{k}}^{\dagger} \end{pmatrix}, \tag{7}$$

with which the model Hamiltonian can be rewritten as

$$\mathcal{H} = \frac{1}{2} \sum_{\mathbf{k}} \Psi_{\mathbf{k}}^{\dagger} (\xi_{\mathbf{k}} \sigma_z) \Psi_{\mathbf{k}} + \frac{1}{2\lambda} \sum_{\mathbf{q}} \hat{\rho}_{\mathbf{q}}^{\dagger} \hat{\rho}_{\mathbf{q}}, \tag{8}$$

where

$$\hat{\rho}_{\mathbf{q}} \equiv \lambda \sum_{\mathbf{k}} \Gamma^*(\mathbf{k}) b_{\mathbf{k}\mathbf{q}} = \lambda \sum_{\mathbf{k}} \Psi_{\mathbf{k}-\frac{\mathbf{q}}{2}}^{\dagger} \Gamma^*(\mathbf{k}) \sigma_- \Psi_{\mathbf{k}+\frac{\mathbf{q}}{2}} \tag{9}$$

is a generalized density operator for a pair of fermions and σ_z and $\sigma_{\pm} = (\sigma_x \pm \sigma_y)/2$ are the Pauli matrices. In the following, we first solve the model Hamiltonian at the mean-field level and then include Gaussian pair fluctuations on top of the mean-field solution.

A. Mean-field theory

The superfluid phase is characterized by a nonzero (real) pairing order parameter Δ at zero center-of-mass momentum $\mathbf{q} = 0$, i.e.,

$$\hat{\rho}_{\mathbf{q}} = \Delta\delta_{\mathbf{q},\mathbf{0}} + \Delta_{\mathbf{q}}, \tag{10}$$

where $\Delta_{\mathbf{q}}$ is the pair fluctuation field around the order parameter. Inserting this decoupling into the model Hamiltonian, we obtain

$$\mathcal{H} = \mathcal{H}_{\rm MF} + \frac{1}{2\lambda}\sum_{\mathbf{q}\neq\mathbf{0}} \Delta_{\mathbf{q}}^{\dagger}\Delta_{\mathbf{q}}, \tag{11}$$

$$\mathcal{H}_{\rm MF} = \frac{1}{2}\sum_{\mathbf{k}} \Psi_{\mathbf{k}}^{\dagger}\begin{bmatrix} \xi_{\mathbf{k}} & \Delta\Gamma(\mathbf{k}) \\ \Delta\Gamma^{*}(\mathbf{k}) & -\xi_{\mathbf{k}} \end{bmatrix}\Psi_{\mathbf{k}} - \frac{\Delta^2}{2\lambda}. \tag{12}$$

Here, we neglect the fluctuation field at zero momentum, which gives a vanishing contribution in the thermodynamic limit. The mean-field Hamiltonian can be straightforwardly solved by diagonalizing the 2×2 matrix in Eq. (12). This leads to the following energy of Bogoliubov quasiparticles

$$E_{\mathbf{k}} = \sqrt{\xi_{\mathbf{k}}^2 + \Delta^2|\Gamma(\mathbf{k})|^2}, \tag{13}$$

and quasiparticle wave functions

$$|u_{\mathbf{k}}|^2 = \frac{1}{2}\left(1 + \frac{\xi_{\mathbf{k}}}{E_{\mathbf{k}}}\right), \tag{14}$$

$$|v_{\mathbf{k}}|^2 = \frac{1}{2}\left(1 - \frac{\xi_{\mathbf{k}}}{E_{\mathbf{k}}}\right), \tag{15}$$

$$u_{\mathbf{k}}v_{\mathbf{k}}^{*} = \frac{\Delta\Gamma(\mathbf{k})}{2E_{\mathbf{k}}}. \tag{16}$$

The BCS Green's function

$$\mathcal{G}_0(\mathbf{k}, i\omega_m) = \begin{bmatrix} i\omega_m - \xi_{\mathbf{k}} & -\Delta\Gamma(\mathbf{k}) \\ -\Delta\Gamma^{*}(\mathbf{k}) & i\omega_m + \xi_{\mathbf{k}} \end{bmatrix}^{-1}, \tag{17}$$

where $\omega_m = (2m+1)\pi k_B T$ $(m \in \mathbb{Z})$ is the fermionic Matsubara frequency, is then given by

$$\mathcal{G}_0^{11}(\mathbf{k}, i\omega_m) = \frac{u_{\mathbf{k}}u_{\mathbf{k}}^{*}}{i\omega_m - E_{\mathbf{k}}} + \frac{v_{\mathbf{k}}v_{\mathbf{k}}^{*}}{i\omega_m + E_{\mathbf{k}}}, \tag{18}$$

$$\mathcal{G}_0^{12}(\mathbf{k}, i\omega_m) = \frac{u_{\mathbf{k}}v_{\mathbf{k}}^{*}}{i\omega_m - E_{\mathbf{k}}} - \frac{u_{\mathbf{k}}v_{\mathbf{k}}^{*}}{i\omega_m + E_{\mathbf{k}}}, \tag{19}$$

$$\mathcal{G}_0^{21}(\mathbf{k}, i\omega_m) = \frac{u_{\mathbf{k}}^{*}v_{\mathbf{k}}}{i\omega_m - E_{\mathbf{k}}} - \frac{u_{\mathbf{k}}^{*}v_{\mathbf{k}}}{i\omega_m + E_{\mathbf{k}}}, \tag{20}$$

$$\mathcal{G}_0^{22}(\mathbf{k}, i\omega_m) = \frac{v_{\mathbf{k}}v_{\mathbf{k}}^{*}}{i\omega_m - E_{\mathbf{k}}} + \frac{u_{\mathbf{k}}u_{\mathbf{k}}^{*}}{i\omega_m + E_{\mathbf{k}}}. \tag{21}$$

The pairing order parameter can be determined by minimizing the mean-field thermodynamic potential,

$$\begin{aligned}\Omega_{\rm MF} &= \frac{1}{2}\frac{\Delta^2}{\lambda} + \frac{1}{2}\sum_{\mathbf{k}}(\xi_{\mathbf{k}} - E_{\mathbf{k}}), \\ &= \frac{1}{2}\sum_{\mathbf{k}}\left[\xi_{\mathbf{k}} - E_{\mathbf{k}} - \frac{\Delta^2|\Gamma(\mathbf{k})|^2}{2\epsilon_{\mathbf{k}} - E_b}\right].\end{aligned} \tag{22}$$

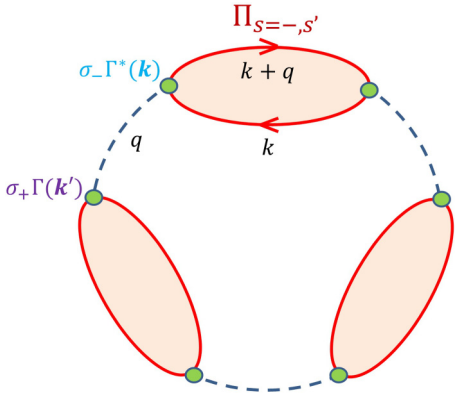

FIG. 1. The third-order ladder diagram considered in the Gaussian pair fluctuation theory. The solid line with arrow represents the 2×2 BCS Green's functions. The dashed line with two vertices indicates the interparticle interaction. There are four types of ladders, $\Pi_{ss'}$, depending on the choice of the interaction vertex: $s = +$ for $\sigma_+\Gamma(\mathbf{k}')$ and $s = -$ for $\sigma_-\Gamma^*(\mathbf{k})$.

Thus, we obtain the gap equation,

$$\sum_{\mathbf{k}}\left[\frac{1}{2E_{\mathbf{k}}} - \frac{1}{2\epsilon_{\mathbf{k}} - E_b}\right]|\Gamma(\mathbf{k})|^2 = 0. \tag{23}$$

At the mean-field level, as mentioned earlier, the chemical potential μ is adjusted to satisfy the mean-field number equation,

$$n = n_F \equiv -\frac{\partial\Omega_{\rm MF}}{\partial\mu} = \frac{1}{2}\sum_{\mathbf{k}}\left(1 - \frac{\xi_{\mathbf{k}}}{E_{\mathbf{k}}}\right). \tag{24}$$

B. Gaussian pair fluctuation theory

We now take into account the fluctuation terms $\Delta_{\mathbf{q}}^{\dagger}\Delta_{\mathbf{q}}/(2\lambda)$ at nonzero center-of-mass momentum. At the lowest Gaussian level, their contribution to the thermodynamic potential can be represented by the ladder (or bubble) diagrams [12,51], one of which (i.e., the third-order diagram) is shown in Fig. 1, where the dashed lines denote the bare interaction $\lambda\Gamma(\mathbf{k})\Gamma^*(\mathbf{k}')$. Following the standard diagrammatic rules [56], an nth-order ladder diagram gives the following contribution to the thermodynamic potential:

$$\begin{aligned}\Omega_{\rm GF}^{(n)} &= \frac{(-1)^{n+1}\lambda^n}{2n}\sum_{\mathcal{Q}}\sum_{s_1,\ldots,s_n'}[\Pi(\mathcal{Q})]_{s_1s_1'}\cdots[\Pi(\mathcal{Q})]_{s_ns_n'} \\ &= \frac{(-1)^{n+1}\lambda^n}{2n}\sum_{\mathcal{Q}}{\rm Tr}\begin{bmatrix} \Pi_{-+}(\mathcal{Q}) & \Pi_{--}(\mathcal{Q}) \\ \Pi_{++}(\mathcal{Q}) & \Pi_{+-}(\mathcal{Q}) \end{bmatrix}^n,\end{aligned} \tag{25}$$

where we have used the short-hand notations $\mathcal{Q} = (\mathbf{q}, i\nu_n)$ with $\nu_n = 2n\pi k_B T$ $(n \in \mathbb{Z})$ being the bosonic Matsubara frequency, and $\sum_{\mathcal{Q}} \equiv k_B T\sum_{i\nu_n}\sum_{\mathbf{q}}$. The subscript $s = -, +$ (or s') of the pair propagator $[\Pi(\mathcal{Q})]_{s,s'}$ stands for the interaction vertices $\sigma_-\Gamma^*(\mathbf{k})$ and $\sigma_+\Gamma(\mathbf{k}')$, respectively. The different choice for s and s' leads to four kinds of ladders and hence

four pair propagators:

$$\Pi_{-+}(\mathcal{Q}) = k_B T \sum_{\mathbf{k}, i\omega_m} |\Gamma(\mathbf{k})|^2 \mathrm{Tr}\left[\sigma_- \mathcal{G}_0\left(\mathbf{k}+\frac{\mathbf{q}}{2}, i\omega_m\right)\sigma_+ \mathcal{G}_0\left(\mathbf{k}-\frac{\mathbf{q}}{2}, i\omega_m - i\nu_n\right)\right], \tag{26}$$

$$\Pi_{--}(\mathcal{Q}) = k_B T \sum_{\mathbf{k}, i\omega_m} [\Gamma^*(\mathbf{k})]^2 \mathrm{Tr}\left[\sigma_- \mathcal{G}_0\left(\mathbf{k}+\frac{\mathbf{q}}{2}, i\omega_m\right)\sigma_- \mathcal{G}_0\left(\mathbf{k}-\frac{\mathbf{q}}{2}, i\omega_m - i\nu_n\right)\right], \tag{27}$$

$\Pi_{++}(\mathcal{Q}) = [\Pi_{--}(\mathcal{Q})]^*$, and $\Pi_{+-}(\mathcal{Q}) = [\Pi_{-+}(\mathcal{Q})]^*$. However, the summation indices $s_1, \ldots, s_n'$ in $\Omega_{\mathrm{GF}}^{(n)}$ cannot take arbitrary values. As each interaction line contains the vertex $\sigma_-\Gamma^*(\mathbf{k})$ and $\sigma_+\Gamma(\mathbf{k}')$ in *pairs*, we must have $s_i' = -s_{i+1}$ for $i = 1, \ldots, n$ (we set $n+1 \to 1$). The summation over the vertex indices therefore leads to the trace of a matrix product, as given in Eq. (25). The contribution of all the ladder diagrams is then readily calculated, by summing over n. We find that

$$\Omega_{\mathrm{GF}}[\mu, \Delta(\mu)] = \frac{1}{2}\sum_{\mathcal{Q}} \mathrm{Tr}\ln\left[-\frac{1}{\lambda} + \begin{pmatrix} \Pi_{-+}(\mathcal{Q}) & \Pi_{--}(\mathcal{Q}) \\ \Pi_{++}(\mathcal{Q}) & \Pi_{+-}(\mathcal{Q}) \end{pmatrix}\right] \equiv \frac{1}{2}\sum_{\mathcal{Q}} \ln\det\begin{bmatrix} M_{11}(\mathcal{Q}) & M_{12}(\mathcal{Q}) \\ M_{21}(\mathcal{Q}) & M_{22}(\mathcal{Q}) \end{bmatrix}, \tag{28}$$

where the explicit expression of $\mathbf{M}(\mathcal{Q})$ is given by

$$M_{11}(\mathcal{Q}) = \sum_{\mathbf{k}} |\Gamma_{\mathbf{k}}(\mathbf{k})|^2 \left[\frac{(u_+u_+^*)(u_-u_-^*)}{i\nu_n - E_+ - E_-} - \frac{(v_+v_+^*)(v_-v_-^*)}{i\nu_n + E_+ + E_-} + \frac{1}{2E_{\mathbf{k}}}\right], \tag{29}$$

$$M_{12}(\mathcal{Q}) = \sum_{\mathbf{k}} [\Gamma^*(\mathbf{k})]^2 \left[\frac{(u_+v_+^*)(u_-v_-^*)}{i\nu_n - E_+ - E_-} - \frac{(u_+v_+^*)(u_-v_-^*)}{i\nu_n + E_+ + E_-}\right], \tag{30}$$

$M_{21}(\mathcal{Q}) = M_{12}^*(\mathcal{Q})$, and $M_{22}(\mathcal{Q}) = M_{11}^*(\mathcal{Q})$. Here, we abbreviate $u_\pm \equiv u_{\mathbf{q}/2\pm\mathbf{k}}$, $v_\pm \equiv v_{\mathbf{q}/2\pm\mathbf{k}}$, and $E_\pm \equiv E_{\mathbf{q}/2\pm\mathbf{k}}$, and rewrite the bare interaction strength λ using Eqs. (6) and (23). In Ω_{GF}, we have exchanged the order of the trace and "ln" operators, which gives rise to the determinant of the pair propagator matrix. Moreover, the summation over the bosonic Matsubara frequency $i\nu_n$ diverges, as a result of $M_{11}(\mathcal{Q}) \sim \nu_n^{1/2}$ in the limit of $\nu_n \to \infty$. This divergence can be formally cured by imposing a convergence factor and converting the summation into a contour integral along the real axis [51]. In practice, it is more convenient to adopt an interesting trick proposed by Diener and his co-workers at zero temperature [52]. We define the regular part of the pair propagators $M_{11}(\mathcal{Q})$ and $M_{22}(\mathcal{Q})$ [52,54]:

$$M_{11}^C = \sum_{\mathbf{k}} |\Gamma(\mathbf{k})|^2 \left[\frac{(u_+u_+^*)(u_-u_-^*)}{i\nu_n - E_+ - E_-} + \frac{1}{2E_{\mathbf{k}}}\right] \tag{31}$$

and $M_{22}^C(\mathcal{Q}) = [M_{11}^C(\mathcal{Q})]^*$. It is easy to check that $M_{11}^C(\mathbf{q}, i\nu_n \to z)$ has no singularities or zeros (i.e., poles and branch cuts) in the left-half complex plane of $\mathrm{Re}\, z < 0$, as a result of $|u_\pm|^2 \leqslant 1$ and $E_+ + E_- \geqslant 2E_{\mathbf{k}}$. At zero temperature, we obtain

$$k_B T \sum_{i\nu_n} \ln M_{11}^C(\mathcal{Q}) = k_B T \sum_{i\nu_n} \ln M_{22}^C(\mathcal{Q}) = 0, \tag{32}$$

after writing them in terms of a standard contour integral [52]. Therefore, we arrive at [52]

$$\Omega_{\mathrm{GF}} = \frac{1}{2}\sum_{\mathbf{q}} k_B T \sum_{i\nu_n} \ln \frac{[M_{11}M_{22} - M_{12}M_{21}](\mathcal{Q})}{M_{11}^C(\mathcal{Q})M_{22}^C(\mathcal{Q})}. \tag{33}$$

A further simplification can be made by noticing that, at zero temperature ($T \to 0$), we may take $\nu_n \to \omega$ as a continuous variable and rewrite the summation $k_B T \sum_{i\nu_n}$ in the form of an integral, $\int_{-\infty}^{+\infty} d\omega/(2\pi)$ [52,54]. By defining the following five functions [54],

$$M_{11}^C = A(\mathbf{q}, \omega) - i\omega B(\mathbf{q}, \omega), \tag{34}$$

$$M_{11} - M_{11}^C = -\Delta^4 C(\mathbf{q}, \omega) + i\omega\Delta^4 D(\mathbf{q}, \omega), \tag{35}$$

$$M_{12} = 2\Delta^2 F(\mathbf{q}, \omega), \tag{36}$$

the Gaussian fluctuation contribution to the thermodynamic potential finally takes the form

$$\Omega_{\mathrm{GF}}[\mu, \Delta(\mu)] = \int_0^\infty \frac{d\omega}{2\pi}\sum_{\mathbf{q}} \ln\left[1 - 2\Delta^4(\mu)\frac{AC + \omega^2 BD + 2F^2}{A^2 + \omega^2 B^2} + \Delta^8(\mu)\frac{C^2 + \omega^2 D^2}{A^2 + \omega^2 B^2}\right]. \tag{37}$$

The explicit form of the five functions is given by

$$A(\mathbf{q},\omega) = -\frac{1}{4}\sum_{\mathbf{k}} |\Gamma(\mathbf{k})|^2 \left[\left(\frac{1}{E_+}+\frac{1}{E_-}\right)\frac{(E_++\xi_+)(E_-+\xi_-)}{\omega^2+(E_++E_-)^2} - \frac{2}{E}\right], \tag{38}$$

$$B(\mathbf{q},\omega) = +\frac{1}{4}\sum_{\mathbf{k}} |\Gamma(\mathbf{k})|^2 \frac{1}{E_+E_-}\frac{(E_++\xi_+)(E_-+\xi_-)}{\omega^2+(E_++E_-)^2}, \tag{39}$$

$$C(\mathbf{q},\omega) = +\frac{1}{4}\sum_{\mathbf{k}} |\Gamma(\mathbf{k})|^2 \left|\Gamma\left(\frac{\mathbf{q}}{2}+\mathbf{k}\right)\right|^2 \left|\Gamma\left(\frac{\mathbf{q}}{2}-\mathbf{k}\right)\right|^2 \left(\frac{1}{E_+}+\frac{1}{E_-}\right)\frac{1}{(E_++\xi_+)(E_-+\xi_-)}\frac{1}{\omega^2+(E_++E_-)^2}, \tag{40}$$

$$D(\mathbf{q},\omega) = +\frac{1}{4}\sum_{\mathbf{k}} |\Gamma(\mathbf{k})|^2 \left|\Gamma\left(\frac{\mathbf{q}}{2}+\mathbf{k}\right)\right|^2 \left|\Gamma\left(\frac{\mathbf{q}}{2}-\mathbf{k}\right)\right|^2 \frac{1}{E_+E_-}\frac{1}{(E_++\xi_+)(E_-+\xi_-)}\frac{1}{\omega^2+(E_++E_-)^2}, \tag{41}$$

$$F(\mathbf{q},\omega) = -\frac{1}{4}\sum_{\mathbf{k}} [\Gamma^*(\mathbf{k})]^2 \Gamma\left(\frac{\mathbf{q}}{2}+\mathbf{k}\right)\Gamma\left(\frac{\mathbf{q}}{2}-\mathbf{k}\right)\left(\frac{1}{E_+}+\frac{1}{E_-}\right)\frac{1}{\omega^2+(E_++E_-)^2}. \tag{42}$$

For our case with a chiral p-wave interaction (i.e., $\Gamma(k) \propto k_x + ik_y$), one may show that the above five functions do not depend on the polar angle of $\mathbf{q}$ (see Appendix B), and thus we can simply set $\mathbf{q} = q\mathbf{e}_x$ in the $\mathbf{k}$-integration of A, B, C, D, and F. This reduces the calculation of $\Omega_{\rm GF}$ to a four-dimensional integration (over ω, $q = |\mathbf{q}|$, $k = |\mathbf{k}|$, and $\varphi_{\mathbf{k}}$).

For a given chemical potential μ, once the fluctuation thermodynamic potential $\Omega_{\rm GF}$ is obtained, we calculate the number of Cooper pairs, n_B, by using numerical differentiation:

$$2n_B = -\frac{\partial\Omega_{\rm GF}[\mu,\Delta(\mu)]}{\partial\mu}. \tag{43}$$

Within the GPF theory, we then adjust the chemical potential to satisfy the number equation $n = n_F + 2n_B$. It is worth noting that the pairing gap $\Delta(\mu)$ is always determined at the mean-field level by using the gap equation, Eq. (23), in order to have a gapless Goldstone phonon mode [51,52].

IV. RESULTS AND DISCUSSIONS

For the convenience of numerical calculations we take the Fermi wave vector k_F as the units of the wave vectors (k, q), and the Fermi energy $\varepsilon_F = \hbar^2k_F^2/(2m) = 2\pi\hbar^2 n/m$ as the units of energy and temperature. This is equivalent to setting $2m = \hbar = k_B = 1$. In the following, we mainly choose a cutoff momentum $k_0 = 30k_F$ and the dependence of various properties on k_0 is briefly discussed at the end of the section.

A. Equation of state

In Fig. 2, we report the chemical potential μ as a function of the interaction strength E_b, predicted by the mean-field theory and GPF theory. To clearly show the many-body effect, we have subtracted the two-body contribution from the bound state when the scattering energy $E_b < 0$, which takes the form $-\varepsilon_B/2 \equiv -\max(-E_b, 0)/2$. In the BCS limit ($E_b \gg \varepsilon_F$), both mean-field and GPF theories predict $\mu \to \varepsilon_F$, as expected. However, towards the BEC limit ($E_b \ll -\varepsilon_F$), they show entirely different behavior.

In the BEC limit we anticipate that the system may turn into a weakly interacting Bose condensate of composite Cooper pairs of mass $m_B = 2m$, with a bosonic chemical potential given by

$$\mu_B = 2\mu + \varepsilon_B \simeq g_B n_B, \tag{44}$$

where $n_B \simeq n/2$ and g_B is the strength of the interaction between two Cooper pairs. Physically, g_B should decrease as we move to the BEC limit. Using the relation $\varepsilon_F = 2\pi\hbar^2 n/m$, we obtain that

$$g_B \simeq \left(\frac{8\pi\hbar^2}{m}\right)\frac{\mu+\varepsilon_B/2}{\varepsilon_F}. \tag{45}$$

Thus, we observe from Fig. 2 that the mean-field theory incorrectly predicts an increasing pair-pair interaction strength when we approach the BEC limit, while the GPF theory gives a *smaller* pair-pair interaction,

$$g_{B,\rm GF} \simeq 0.032\left(\frac{8\pi\hbar^2}{m}\right) \simeq 1.6\frac{\hbar^2}{m_B}, \tag{46}$$

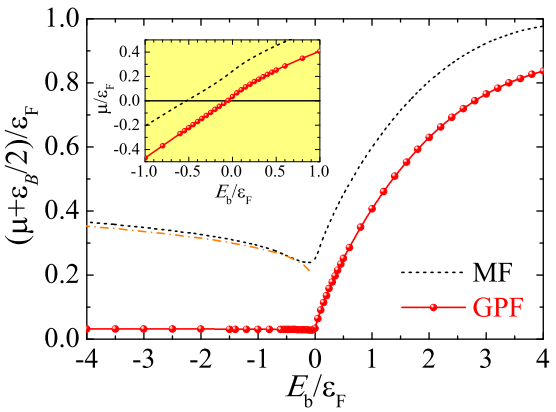

FIG. 2. The chemical potential μ as a function of the scattering energy E_b, calculated by using the mean-field theory (dashed line) and GPF theory (solid line with circles). The dot-dashed line shows the asymptotic behavior in the BEC limit predicted by the mean-field theory in Eq. (47), which corresponds to a constant molecular scattering length for composite bosons. In the main figure, we have subtracted the contribution from the two-body bound state with the binding energy $\varepsilon_B \equiv \max(-E_b, 0)$. The inset highlights the chemical potential near the topological phase transition (i.e., $\mu \sim 0$ or $E_b \sim 0$). Here, we take a cutoff momentum $k_0 = 30k_F$.

which is essentially independent of the scattering energy E_b [57].

In the mean-field theory, the pair-pair interaction strength can be analytically calculated using a Ginzburg-Landau free energy functional for the pair fluctuation field $\Delta_{\mathbf{q}}$ (see Appendix C). We find that

$$g_{B,\mathrm{MF}} = \frac{16\pi\hbar^2}{m}\frac{[\ln\eta + 2\eta^{-1} - \eta^{-2}/2 - 3/2]}{(\ln\eta + \eta^{-1} - 1)^2}, \tag{47}$$

where $\eta = \hbar^2 k_0^2/(m|E_b|) + 1$. As $\eta \gg 1$ for the parameters in Fig. 2, to a good approximation we have

$$g_{B,\mathrm{MF}} \simeq \frac{16\pi\hbar^2}{m}\frac{1}{\ln\left[\hbar^2 k_0^2/(m|E_b|)\right]}, \tag{48}$$

which explains the wrong behavior of stronger pair-pair interaction as we decrease E_b (see the dot-dashed line in Fig. 2).

Quite generally, the mean-field theory breaks down in two dimensions due to enhanced quantum fluctuations. This is already known for an s-wave Fermi superfluid [54], where the mean-field theory predicts a *constant* pair-pair interaction strength of $4\pi\hbar^2/m$, instead of a much smaller and chemical-potential-dependent coupling strength. The renormalization of the pair-pair interaction due to quantum fluctuations is well captured by our GPF theory. Indeed, in an s-wave Fermi superfluid the GPF theory is reliable in predicting an accurate molecular scattering length for composite bosons [54], in good agreement with the exact four-body calculation and diffusion quantum Monte Carlo (QMC) simulation. In our case of a chiral p-wave Fermi superfluid, we anticipate that the GPF theory will similarly lead to a reliable result for the pair-pair interaction strength g_B. Unfortunately, unlike the s-wave Fermi superfluid, the existence of the regularization function $\Gamma(\mathbf{k})$ makes it infeasible to derive an analytic expression for g_B. In future studies, the QMC calculation of the ground-state energy of the system or the exact solution of four resonantly p-wave interacting fermions in two dimensions would be very useful to understand the smaller and constant pair-pair interaction strength g_B, as predicted by our GPF theory.

Let us now consider the intermediate coupling regime near zero scattering energy $E_b = 0$, where the chemical potential μ changes sign and the system is expected to undergo a topological phase transition. In sharp contrast to the s-wave case, where μ evolves rather smoothly, here we find a dramatic change in the slope of the quantity $\mu + \varepsilon_B/2$ at $E_b \sim 0$ or $\mu \sim 0$. This nonanalytic feature at the topological phase transition has been noticed in previous mean-field studies [30,35,39] and we see that quantum fluctuations make it even more pronounced.

Figure 3 presents the evolution of the pairing order parameter Δ as a function of the scattering energy E_b, calculated using the mean-field theory (dashed line) and the GPF theory (solid line with circles). Away from the BCS limit, the pairing gap is significantly reduced by quantum fluctuations. In particular, at resonance, the pairing gap is about a quarter of the Fermi energy, $\Delta \sim 0.25\varepsilon_F$. There is an apparent dip at the topological phase transition, as a result of the nonanalyticity of the thermodynamics at the transition.

Theoretically, the significance of quantum fluctuations can be most easily recognized from the evolution of the number

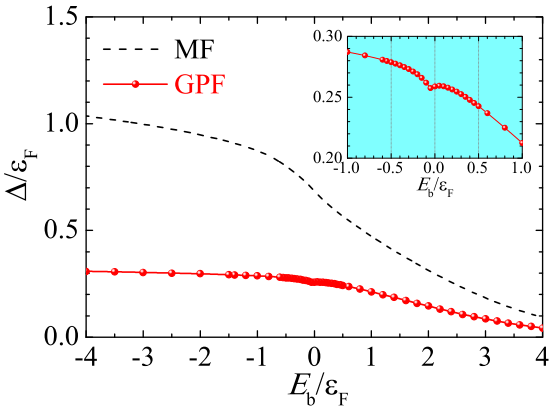

FIG. 3. The pairing gap Δ as a function of the scattering energy E_b, predicted by using the mean-field theory (dashed line) and GPF theory (solid line with circles). The inset highlights the kink in the pairing gap near the topological phase transition (i.e., $E_b \sim 0$). Here, we take a cutoff momentum $k_0 = 30k_F$.

of Cooper pairs, n_B, as a function of the scattering energy E_b, as shown in Fig. 4. We find a rapid increase in n_B when we move to the topological phase-transition point from the BCS limit. Upon reaching the transition, the dependence of the number of Cooper pairs on the scattering energy becomes nearly flat. Once again, this may be viewed as an indication of the nonanalyticity at the topological phase transition.

In experiments, on the other hand, the nonanalyticity of the thermodynamic functions at the transition may be probed by measuring the *homogeneous* pressure equation of state through the density distribution of a harmonically trapped resonant p-wave Fermi superfluid [58]. In Fig. 5, we report the pressure P, normalized to its noninteracting value $P_0 = n\varepsilon_F/2$, as a function of the scattering energy E_b, calculated with the mean-field theory and the GPF theory. The pressure P shows almost the same scattering energy dependence as the chemical potential, with a clear kink at the topological phase transition. Therefore, the observation of this kink may be regarded as an *indirect* proof of the topological phase transition [59]. Moreover, the measurement of the small and nearly constant pressure on the BEC side will be useful

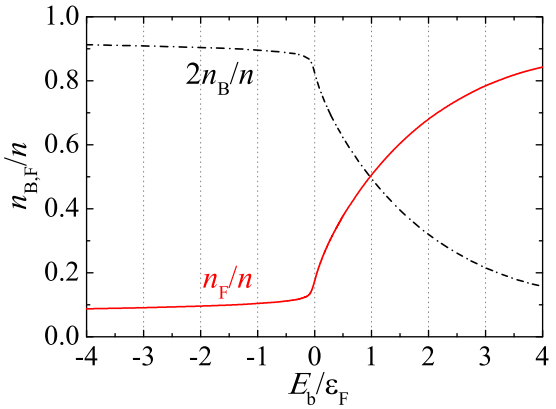

FIG. 4. The fraction of fermions n_F/n (solid line) and Cooper pairs n_B/n (dashed line), as a function of the scattering energy E_b. Here, we take a cutoff momentum $k_0 = 30k_F$.

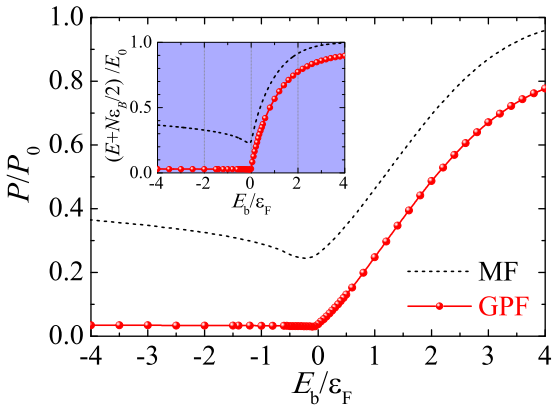

FIG. 5. The pressure (main figure) and total energy (inset), as a function of the scattering energy E_b, predicted by using the mean-field theory (dashed line) and GPF theory (solid line with circles). The pressure and energy are normalized with respect to the ideal gas values $P_0 = n\varepsilon_F/2$ and $E_0 = N\varepsilon_F/2$, respectively. Here, N is the total number of particles. For the total energy, we have subtracted the contribution from the two-body bound state, $-N\varepsilon_B/2$. As before, we take a cutoff momentum $k_0 = 30k_F$.

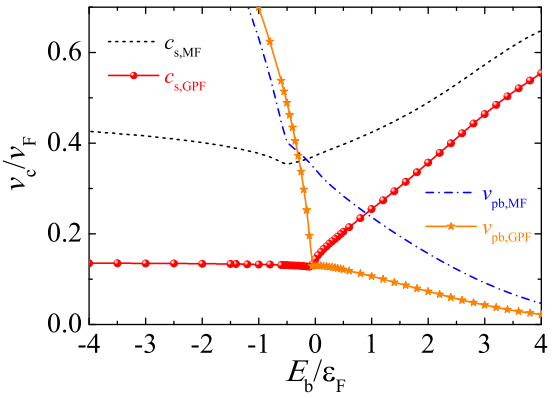

FIG. 6. The sound velocity and pair-breaking velocity, as a function of the scattering energy E_b, predicted by using the mean-field theory (dashed line or dash-dotted line) and GPF theory (solid line with circles or stars). As the scattering energy decreases (or the interaction strength increases), the critical velocity $v_c = \max\{v_{pb}, c_s\}$ slowly increases. Here, we take a cutoff momentum $k_0 = 30k_F$.

to clarify the nature of the resulting weak-interacting Bose condensate.

To conclude this section, it is worth noting a recent study of the same system by Jiang and Zhou [50], based on a two-channel model for a broad p-wave resonance. In that study, quantum fluctuations from selected two-loop diagrams are found to destabilize the system at the resonance, in disagreement with our finding of a stable Fermi superfluid at all interaction strengths. This discrepancy is unlikely from the different model Hamiltonian (i.e., one channel vs two channel), since the one-channel model and two-channel model are known to give the same description for a broad Feshbach resonance [60,61]. It should come from the treatment of quantum fluctuations at different levels. The GPF treatment presented in this work, when it is generalized to the two-channel model [62], includes the two-loop diagrams selected by Jiang and Zhou [50,63]. Moreover, it may pick up a set of marginal diagrams containing higher-order loops, within the ladder or bubble approximation. A future GPF study of the two-channel model for a resonantly interacting p-wave Fermi superfluid will be useful to clarify the discrepancy and to provide more accurate results for a narrow Feshbach resonance.

B. Critical velocity for superfluidity

A superfluid loses its superfluidity when it moves faster than a critical velocity. For an s-wave Fermi superfluid, the critical velocity in the BCS and BEC limits is given by the pair-breaking velocity and sound velocity, respectively, and exhibits a maximum in between [52]. A maximum critical velocity at the resonance emphasizes the stability of a strongly interacting Fermi superfluid [64].

The situation for a p-wave Fermi superfluid seems to be a bit different. In Fig. 6, we present the sound velocity determined from the equation of state,

$$c_s = \left[\frac{n}{m}\frac{\partial\mu}{\partial n}\right]^{1/2} = \left[\frac{n}{m}\left(-\frac{\partial^2\Omega}{\partial\mu^2}\right)^{-1}\right]^{1/2}, \tag{49}$$

and the pair-breaking velocity calculated by using the Landau criterion,

$$v_{pb} = \min_{\{\mathbf{k}\}}\frac{E_{\mathbf{k}}}{|k|} \simeq \begin{cases} \Delta & \text{if } \mu \geqslant 0 \\ \sqrt{\Delta^2 - 4\mu} & \text{if } \mu < 0. \end{cases} \tag{50}$$

In both mean-field and GPF frameworks, the resulting critical velocity $v_c = \max\{v_{pb}, c_s\}$ roughly increases with decreasing scattering energy E_b. In particular, on the BEC side, the GPF result of the critical velocity becomes nearly flat, consistent with a constant pair-pair interaction strength observed earlier. Typically, the critical velocity at resonance is about $0.1v_F$, smaller than that of an s-wave Fermi superfluid [55,65]. This means that a p-wave Fermi superfluid could be more easily destroyed than its s-wave counterpart.

C. BKT transition temperature

In two dimensions, the transition to a superfluid state at finite temperature is governed by the BKT mechanism [66,67]. The BKT critical temperature T_c of a chiral p-wave Fermi superfluid was considered in the previous studies by using the mean-field theory [39]. Here, we determine T_c with the inclusion of quantum fluctuations.

For this purpose, we need to calculate the superfluid density n_s and then determine T_c using the so-called Thouless-Nelson criterion [68],

$$k_B T_c = \frac{\pi\hbar^2}{8m} n_s(T_c), \tag{51}$$

or equivalently,

$$\frac{T_c}{T_F} = \frac{1}{16}\frac{n_s(T_c)}{n}. \tag{52}$$

A full calculation of superfluid density n_s within the GPF framework is numerically involved. Here, we follow the idea

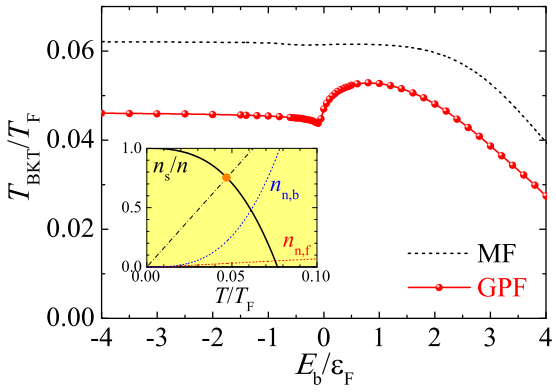

FIG. 7. The BKT transition temperature, calculated by using the mean-field theory (dashed line) and GPF theory (solid line with circles), as a function of the scattering energy E_b. The inset shows the normal density fractions contributed by fermions, $n_{n,f}/n$, and by pairs, $n_{n,b}/n$, and the superfluid density fraction $n_s/n = 1 - n_{n,f}/n - n_{n,b}/n$ at zero scattering energy $E_b = 0$. The cross point between the superfluid fraction n_s/n and the line $16T/T_F$ determines the BKT temperature at $E_b = 0$. Here, we take a cutoff momentum $k_0 = 30k_F$.

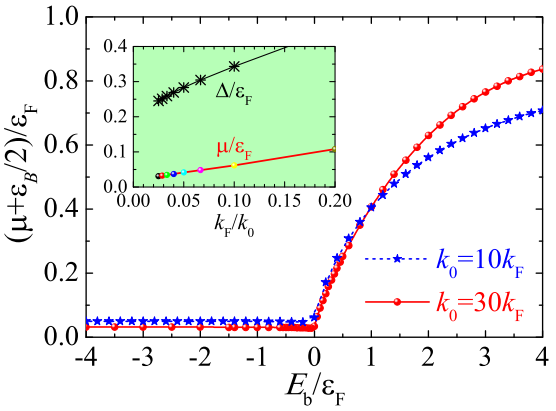

FIG. 8. The chemical potential μ (with the two-body bound-state contribution subtracted) as a function of the scattering energy E_b, at two cutoff momenta $k_0 = 10k_F$ (dashed line with stars) and $k_0 = 30k_F$ (solid line with circles). The inset shows the chemical potential μ and pairing gap Δ at the zero scattering energy $E_b = 0$, as a function of the inverse cutoff momentum k_0^{-1}. All the results are predicted by using the GPF theory.

by Bighin and Salasnich to approximately calculate the superfluid density using the standard Landau formalism [55]. This provides an approximate but convenient way to include quantum fluctuations [55,65].

To apply the Landau formalism, we assume that the low-energy excitations of the resonantly interacting p-wave superfluid are well described by quasiparticles. This assumption is excellent in both BCS and BEC limits. Therefore, we anticipate that it may also give some qualitative predictions near resonance. Following Landau's quasiparticle picture [69], the densities of the normal fluid, due to single-particle fermionic excitations and collective bosonic excitations, are respectively given by

$$n_{n,f} = -\frac{\hbar^2}{m}\sum_{\mathbf{k}}\frac{\mathbf{k}^2}{2}\frac{\partial}{\partial E_{\mathbf{k}}}\left(\frac{1}{e^{E_{\mathbf{k}}/k_BT}+1}\right), \tag{53}$$

$$n_{n,b} = -\frac{\hbar^2}{m}\sum_{\mathbf{q}}\frac{\mathbf{q}^2}{2}\frac{\partial}{\partial \omega_{\mathbf{q}}}\left(\frac{1}{e^{\omega_{\mathbf{q}}/k_BT}-1}\right), \tag{54}$$

where we approximate that, as a rough estimation, the fermionic excitations have the energy spectrum of $E_{\mathbf{k}}$ and the bosonic excitations have phonon dispersion $\omega_{\mathbf{q}} \simeq c_s q$. The superfluid density n_s then takes the form

$$n_s = n - n_{n,f} - n_{n,b}. \tag{55}$$

At resonance, the normal densities due to fermionic and bosonic excitations, $n_{n,f}$ and $n_{n,b}$, and the superfluid density n_s are shown in the inset of Fig. 7. We find that the bosonic degree of freedom gives the dominant contribution to the superfluid density and hence leads to a reduced BKT critical temperature. Indeed, the mean-field theory predicts a nearly saturated critical temperature $T_c = T_F/16 \sim 0.06T_F$ at resonance, while our GPF theory with Landau formalism for superfluid density gives a smaller critical temperature $T_c \sim 0.04T_F$.

In the main figure of Fig. 7, we present the evolution of the BKT critical temperature T_c as a function of the scattering energy E_b. It exhibits a bump near the resonance with a maximum $T_{c,\max} \simeq 0.052T_F$ at $E_b \sim \varepsilon_F$. The cusp at $E_b \simeq 0$ may be viewed as a clear demonstration of the nonanalyticity of the finite temperature thermodynamics at the topological phase transition. Towards the BEC limit, we find that the BKT critical temperature saturates to $T_c \sim 0.047T_F$.

This smaller BKT critical temperature, compared with the mean-field prediction of $T_c = 0.625T_F$, could be understood using the BKT theory of a 2D interacting Bose gas, for which the Monte Carlo simulation predicts

$$k_BT_c = \frac{2\pi n_B}{m_B \ln[\xi\hbar^2/(m_B g_B)]}, \tag{56}$$

where $\xi = 380 \pm 3$ [70]. By recalling $\varepsilon_F = 2\pi\hbar^2 n/m = 8\pi\hbar^2 n_B/m_B$ and using $g_B \simeq 1.6\hbar^2/m_B$ in Eq. (46), we find that

$$T_c \simeq \frac{1}{4\ln(380/1.6)}\frac{\varepsilon_F}{k_B} \simeq 0.046T_F, \tag{57}$$

which is consistent with our GPF prediction of $T_c \sim 0.047T_F$.

D. The dependence on the cutoff momentum k_0

We now turn to discuss the cutoff momentum dependence of our results. In the main figure of Fig. 8, we compare the chemical potentials at the BEC-BCS evolution at two cutoff momenta, $k_0 = 10k_F$ (dashed line with stars) and $k_0 = 30k_F$ (solid line with circles). A factor of 3 reduction in the cutoff momentum does not lead to any changes at the qualitative level. In the inset, we highlight the cutoff momentum dependence of the chemical potential and pairing gap at the resonance. We do not find singular behaviors as we increase the cutoff momentum and extend it towards infinity. Therefore, although a cutoff momentum k_0 is necessary to make the p-wave interaction renormalizable (for dimensions $d \geqslant 2$),

we may still have some universal behaviors that are weakly (i.e., logarithmically) dependent on k_0^{-1}.

V. CONCLUSIONS AND OUTLOOKS

In conclusion, we have theoretically investigated the consequence of quantum fluctuations in a resonantly interacting p-wave Fermi superfluid in two dimensions at the BEC-BCS evolution, using the Gaussian pair fluctuation theory. We have found that the zero-temperature equations of state, the critical velocity for superfluidity, and the BKT critical temperature are strongly renormalized by quantum fluctuations, and their nonanalyticity at the topological phase transition is greatly enhanced. Experimentally, this nonanalyticity could be best probed by measuring the pressure equation of state at zero temperature, which shows an apparent kink near resonance, and the BKT critical temperature, which exhibits a bump and then a cusp structure. Although the p-wave Fermi superfluid seems to be delicate in superfluidity compared with its s-wave counterpart due to a smaller critical velocity, it is thermodynamically stable at all interaction strengths, in disagreement with a previous theoretical study [50], which takes into account quantum fluctuations at the level of two-loop diagrams.

For p-wave interacting fermions in two dimensions, Nishida and co-workers recently predicted the existence of a series of three-particle bound states, the so-called super-Efimov states [71]. The impact of these super-Efimov states to the many-body properties (i.e., superfluidity) of the system remains to be understood. It will be an interesting research topic to be explored in future studies.

ACKNOWLEDGMENTS

This research was supported by Australian Research Council (ARC) Programs No. FT130100815 and DP170104008 (H.H.), No. DE180100592 (J.W.), and No. FT140100003 and DP180102018 (X.J.L.), the National Key R&D Program of China (Grant No. 2018YFA0306503) (L.H.), and the National Natural Science Foundation of China, Grant No. 11775123 (L.H.).

APPENDIX A: TWO-PARTICLE SCATTERING

We use a separable interaction potential to characterize the chiral p-wave interatomic interaction:

$$V_{\mathbf{k}\mathbf{k}'} = \lambda \Gamma(\mathbf{k})\Gamma^*(\mathbf{k}'), \tag{A1}$$

$$\Gamma(\mathbf{k}) = \frac{(k/k_1)}{[1+(k/k_0)^{2n}]^{3/2}} e^{i\varphi_{\mathbf{k}}}, \tag{A2}$$

where k_1—set to be k_F in numerical calculations—is a characteristic momentum that makes $\Gamma(\mathbf{k})$ dimensionless, k_0 is a large-momentum cutoff, and $\varphi_{\mathbf{k}}$ is the polar angle of $\mathbf{k}$ in 2D momentum space. We use the exponent n to control the shape of the regularization function $\Gamma(\mathbf{k})$. In the large-n limit, effectively we have a step function.

To obtain the two-body scattering amplitude, we consider the following two-body T-matrix in vacuum:

$$T(\mathbf{k},\mathbf{k}';E_+) = t(E_+)\Gamma(\mathbf{k})\Gamma^*(\mathbf{k}'), \tag{A3}$$

$$\frac{1}{t(E_+)} = \frac{1}{\lambda} + \sum_{\mathbf{k}''} \frac{|\Gamma(\mathbf{k}'')|^2}{2\epsilon_{\mathbf{k}''} - E_+}, \tag{A4}$$

where $k' = |\mathbf{k}'| = k$ and $E_+ = \hbar^2 k^2/m + i0^+$. The analytic form of the scattering amplitude or $t(E_+)$ in the low-energy limit (i.e., $k \to 0$) should be independent of the detailed regularization function. Therefore, we may simply use a step function (i.e., $n \to \infty$). By introducing a new variable $x = (k'')^2$, we find that

$$\frac{1}{t(E_+)} = \frac{1}{\lambda} + \frac{m}{4\pi\hbar^2 k_1^2}\int_0^{k_0^2} dx \frac{x}{x-\tilde{E}_+}, \tag{A5}$$

where $\tilde{E}_+ = k^2 + i0^+$. This leads to ($\tilde{E} = k^2$)

$$\frac{1}{t(E_+)} = \frac{1}{\lambda} + \frac{m}{4\pi\hbar^2 k_1^2}\left[k_0^2 + \tilde{E}\ln\left(\frac{k_0^2}{\tilde{E}} - 1\right) + i\pi\tilde{E}\right]. \tag{A6}$$

By taking the low-energy limit $k \to 0$, we arrive at

$$\frac{1}{t(E_+)} = -\frac{m}{4\pi\hbar^2 k_1^2}\left[-\frac{1}{a_p} + \frac{2k^2}{\pi}\ln(R_p k) - ik^2\right], \tag{A7}$$

where $R_p \sim 1/k_0$ is the effective range of the p-wave interaction, the term a_p^{-1} collects all the constants in Eq. (A6) and physically we interpret a_p as the p-wave scattering area in two dimensions. It is easy to see that the full two-body T-matrix is ($k = k'$)

$$T(\mathbf{k},\mathbf{k}';E_+) = e^{i(\varphi_{\mathbf{k}}-\varphi_{\mathbf{k}'})}\left(-\frac{4\hbar^2}{m}\right) \times \left[\frac{kk'}{-a_p^{-1} + (2k^2/\pi)\ln(R_p k) - ik^2}\right]. \tag{A8}$$

According to Levinsen, Cooper, and Gurarie (see Appendix in Ref. [26]), we may define a two-dimensional p-wave scattering amplitude

$$\begin{aligned} f_p(k) &= -\frac{m}{2\hbar^2(2\pi k)^{1/2}} T(\mathbf{k},\mathbf{k};E_+) \\ &= \sqrt{\frac{2}{\pi k}}\frac{k^2}{-a_p^{-1} + (2k^2/\pi)\ln(R_p k) - ik^2} \\ &= \frac{1}{g_p(k) - i(\pi k/2)^{1/2}}, \end{aligned} \tag{A9}$$

where

$$g_p(k) = \sqrt{\frac{\pi k}{2}}\frac{-a_p^{-1} + (2k^2/\pi)\ln(R_p k)}{k^2} \tag{A10}$$

is a real function of k. The p-wave scattering amplitude may also be written in terms of the phase shift $\delta_p(k)$ [26]:

$$f_p(k) = \frac{1}{i\sqrt{2\pi k}}(e^{2i\delta_p} - 1) = \sqrt{\frac{2}{\pi k}}\frac{1}{\cot\delta_p - i}, \tag{A11}$$

where the phase shift satisfies

$$k^2 \cot \delta_p(k) = -\frac{1}{a_p} + \frac{2k^2}{\pi} \ln(R_p k) + \cdots . \tag{A12}$$

We note that the relation between the scattering amplitude $f_p(k)$ and phase shift $\delta_p(k)$ defined in Eq. (A11) is slightly different from that derived by solving the two-body problem (see Eq. (11) in Ref. [44]).

APPENDIX B: THE STRUCTURE OF THE FUNCTIONS *A*, *B*, *C*, *D*, AND *F*

Here we demonstrate that the functions A, B, C, D, and F do not depend on the direction of $\mathbf{q}$, and thus we may simply set $\mathbf{q} = q\mathbf{e}_x$ in numerical calculations. Actually, this is pretty clear for A, B, C, and D, since the factor $|\Gamma(\mathbf{k})|$ does not depend on the polar angle $\varphi_{\mathbf{k}}$. All the integral functions therefore depend on the angle between $\mathbf{q}$ and $\mathbf{k}$ only, or more precisely $\cos(\varphi_{\mathbf{k}} - \varphi_{\mathbf{q}})$. For the function F, we now need to check explicitly that the factor

$$P = \Gamma^*(\mathbf{k})\Gamma^*(\mathbf{k})\Gamma\left(\frac{\mathbf{q}}{2} + \mathbf{k}\right)\Gamma\left(\frac{\mathbf{q}}{2} - \mathbf{k}\right) \tag{B1}$$

also depends on $\varphi_{\mathbf{k}} - \varphi_{\mathbf{q}}$ only. We may also explicitly show that F is a real function. For this purpose, we examine the following product:

$$P = \tilde{P}(k, q; \varphi_{\mathbf{k}} - \varphi_{\mathbf{q}}) e^{-i2\varphi_{\mathbf{k}}} \left[\left(\frac{q_x}{2} + k_x\right) + i\left(\frac{q_y}{2} + k_y\right)\right]\left[\left(\frac{q_x}{2} - k_x\right) + i\left(\frac{q_y}{2} - k_y\right)\right], \tag{B2}$$

$$= \tilde{P}(k, q; \varphi_{\mathbf{k}} - \varphi_{\mathbf{q}}) e^{-i2\varphi_{\mathbf{k}}} \left[\frac{(q_x^2 - q_y^2)}{4} - (k_x^2 - k_y^2) + i2\left(\frac{q_x q_y}{4} - k_x k_y\right)\right], \tag{B3}$$

$$= \tilde{P}(k, q; \varphi_{\mathbf{k}} - \varphi_{\mathbf{q}})[\cos 2\varphi_{\mathbf{k}} - i \sin 2\varphi_{\mathbf{k}}]\left[\left(\frac{q^2}{4}\cos 2\varphi_{\mathbf{q}} - k^2 \cos 2\varphi_{\mathbf{k}}\right) + i\left(\frac{q^2}{4}\sin 2\varphi_{\mathbf{q}} - k^2 \sin 2\varphi_{\mathbf{k}}\right)\right], \tag{B4}$$

$$= \tilde{P}(k, q; \varphi_{\mathbf{k}} - \varphi_{\mathbf{q}})\left\{\left[\frac{q^2}{4}\cos(2\varphi_{\mathbf{k}} - 2\varphi_{\mathbf{q}}) - k^2\right] - i\frac{q^2}{4}\sin(2\varphi_{\mathbf{k}} - 2\varphi_{\mathbf{q}})\right\}, \tag{B5}$$

where in the first line of the equation, we have singled out the chiral $p_x + ip_y$ dependence of the regularization function Γ and the function $\tilde{P}$ depends on $\varphi_{\mathbf{k}} - \varphi_{\mathbf{q}}$. It is now clear that, in the calculations of A, B, C, D, and F, $\varphi_{\mathbf{q}}$ can be removed by redefining the angle $\varphi_{\mathbf{k}}$: $\varphi_{\mathbf{k}} - \varphi_{\mathbf{q}} \to \varphi$. The imaginary part of F is strictly zero since

$$\int_0^{2\pi} d\varphi h(\cos\varphi) \sin 2\varphi = 0 \tag{B6}$$

for any function $h(x)$.

APPENDIX C: GINZBURG-LANDAU FREE ENERGY FUNCTIONAL FOR THE PAIR FLUCTUATION FIELD

In the BEC limit, we may derive a Gross-Pitaevskii free energy of composite bosons $\mathcal{S}[\phi(\mathbf{x}, \tau)]$, which takes the form

$$\mathcal{S} = \int dx \left[\phi^*\left(\frac{\partial}{\partial\tau} - \frac{\hbar^2}{2m_B} - \mu_B\right)\phi + \frac{g_B}{2}|\phi|^4\right], \tag{C1}$$

where $m_B = 2m$ is the mass of composite bosons, μ_B is the chemical potential, and g_B is the pair-pair interaction strength, and we abbreviate $x \equiv (\mathbf{x}, \tau)$. To this end, we first consider the Ginzburg-Landau free energy functional for the pair fluctuation field $\Delta(x)$:

$$\tilde{\mathcal{S}} = \int dx \left[\Delta^*\left(a\frac{\partial}{\partial\tau} - b\frac{\hbar^2}{4m} - c\right)\Delta + \frac{d}{2}|\Delta|^4\right], \tag{C2}$$

where the ϕ field can be obtained by rescaling the pair fluctuation field Δ, i.e., $\sqrt{a}\Delta(x) \to \phi(x)$.

Following the seminal work by Sá de Melo, Randeria, and Engelbrecht [13], we determine the coefficients a, b, and c by evaluating the small frequency and momentum expansion of the pair propagator $M_0(\mathbf{q}, i\nu_n)$ in the normal state, which takes the form

$$M_0 = -\frac{1}{2\lambda} + \frac{1}{2}\sum_{\mathbf{k}} \frac{|\Gamma(\mathbf{k})|^2}{i\nu_n + 2\mu - 2\epsilon_{\mathbf{k}} - \hbar^2\mathbf{q}^2/(4m)}. \tag{C3}$$

Using the fact that

$$M_0(\mathbf{q} \to 0, i\nu_n \to 0) \simeq -a(i\nu_n) + b\frac{\hbar^2\mathbf{q}^2}{4m} - c, \tag{C4}$$

we obtain

$$a = b = \frac{1}{2}\sum_{\mathbf{k}} \frac{|\Gamma(\mathbf{k})|^2}{(2\epsilon_{\mathbf{k}} - 2\mu)^2} \tag{C5}$$

and

$$c = \frac{1}{2\lambda} + \frac{1}{2}\sum_{\mathbf{k}} \frac{|\Gamma(\mathbf{k})|^2}{2\epsilon_{\mathbf{k}} - 2\mu}. \tag{C6}$$

In the BEC limit, we have $\mu_B = 2\mu - E_b \to 0^+$. By replacing the bare interaction strength λ with the scattering energy

E_b, it is easy to verify that

$$c \simeq \frac{\mu_B}{2} \sum_{\mathbf{k}} \frac{|\Gamma(\mathbf{k})|^2}{(2\epsilon_{\mathbf{k}} + |E_b|)^2} \simeq \mu_B a. \tag{C7}$$

The integral in a can be worked out in the limit of an infinitely large exponent $n \to \infty$, where $\Gamma(\mathbf{k}) = [(k_x + ik_y)/k_1]\Theta(k_0 - k)$. We find that

$$a = \frac{m^2}{8\pi\hbar^4 k_1^2}\left(\ln\eta + \frac{1}{\eta} - 1\right), \tag{C8}$$

where $\eta = \hbar^2 k_0^2/(m|E_b|) + 1$.

The coefficient d, on the other hand, may be calculated by Taylor-expanding the mean-field thermodynamic potential $\Omega_{\rm MF}$ at small pairing gap $\Delta \sim 0$, i.e.,

$$\Omega_{\rm MF} = -c\Delta^2 + \frac{d}{2}\Delta^4 + \cdots.$$

This leads to

$$c = -\frac{\partial\Omega_{\rm MF}}{\partial\Delta^2} = \frac{1}{2\lambda} + \sum_{\mathbf{k}} \frac{|\Gamma(\mathbf{k})|^2}{2\epsilon_{\mathbf{k}} - 2\mu} \tag{C9}$$

as anticipated, and

$$d = \frac{\partial^2\Omega_{\rm MF}}{\partial(\Delta^2)^2} = \sum_{\mathbf{k}} \frac{|\Gamma(\mathbf{k})|^4}{(2\epsilon_{\mathbf{k}} - 2\mu)^3}. \tag{C10}$$

By replacing -2μ with $|E_b|$ in the equation for d, and performing the integration, we obtain

$$d = \frac{m^3}{4\pi\hbar^6 k_1^4}\left(\ln\eta + \frac{2}{\eta} - \frac{1}{2\eta^2} - \frac{3}{2}\right). \tag{C11}$$

The rescaling of the pair fluctuation field, $\sqrt{a}\Delta(x) \to \phi(x)$, leads to the desired expression for the pair-pair interaction strength,

$$g_B = \frac{d}{a^2} = \frac{16\pi\hbar^2}{m}\frac{[\ln\eta + 2\eta^{-1} - \eta^{-2}/2 - 3/2]}{(\ln\eta + \eta^{-1} - 1)^2}, \tag{C12}$$

which is Eq. (47) in the main text.

[1] V. P. Mineev and K. V. Samokhin, *Introduction to Unconventional Superconductivity* (CRC Press, Boca Raton, FL, 1999).
[2] N. Read and D. Green, Phys. Rev. B **61**, 10267 (2000).
[3] D. A. Ivanov, Phys. Rev. Lett. **86**, 268 (2001).
[4] A. Yu. Kitaev, Ann. Phys. (NY) **303**, 2 (2003).
[5] For a review, see C. Nayak, S. H. Simon, A. Stern, M. Freedman, and S. D. Sarma, Rev. Mod. Phys. **80**, 1083 (2008).
[6] Y. Maeno, H. Hashimoto, K. Yoshida, S. Nishizaki, T. Fujita, J. G. Bednorz, and F. Lichtenberg, Nature (London) **372**, 532 (1994).
[7] For a review, see V. Gurarie and L. Radzihovsky, Ann. Phys. (Amsterdam) **322**, 2 (2007).
[8] I. Bloch, J. Dalibard, and W. Zwerger, Rev. Mod. Phys. **80**, 885 (2008).
[9] S. Giorgini, L. P. Pitaevskii, and S. Stringari, Rev. Mod. Phys. **80**, 1215 (2008).
[10] D. M. Eagles, Phys. Rev. **186**, 456 (1969).
[11] A. J. Leggett, in *Modern Trends in the Theory of Condensed Matter*, edited by A. Pekalski and R. Przystaw (Springer-Verlag, Berlin, 1980).
[12] P. Noziéres and S. Schmitt-Rink, J. Low Temp. Phys. **59**, 195 (1985).
[13] C. A. R. Sá de Melo, M. Randeria, and J. R. Engelbrecht, Phys. Rev. Lett. **71**, 3202 (1993).
[14] C. A. Regal, C. Ticknor, J. L. Bohn, and D. S. Jin, Phys. Rev. Lett. **90**, 053201 (2003).
[15] J. Zhang, E. G. M. van Kempen, T. Bourdel, L. Khaykovich, J. Cubizolles, F. Chevy, M. Teichmann, L. Tarruell, S. J. J. M. F. Kokkelmans, and C. Salomon, Phys. Rev. A **70**, 030702(R) (2004).
[16] K. Günter, T. Stöferle, H. Moritz, M. Köhl, and T. Esslinger, Phys. Rev. Lett. **95**, 230401 (2005).
[17] C. H. Schunck, M. W. Zwierlein, C. A. Stan, S. M. F. Raupach, W. Ketterle, A. Simoni, E. Tiesinga, C. J. Williams, and P. S. Julienne, Phys. Rev. A **71**, 045601 (2005).
[18] J. P. Gaebler, J. T. Stewart, J. L. Bohn, and D. S. Jin, Phys. Rev. Lett. **98**, 200403 (2007).
[19] J. Fuchs, C. Ticknor, P. Dyke, G. Veeravalli, E. Kuhnle, W. Rowlands, P. Hannaford, and C. J. Vale, Phys. Rev. A **77**, 053616 (2008).
[20] Y. Inada, M. Horikoshi, S. Nakajima, M. Kuwata-Gonokami, M. Ueda, and T. Mukaiyama, Phys. Rev. Lett. **101**, 100401 (2008).
[21] T. Nakasuji, J. Yoshida, and T. Mukaiyama, Phys. Rev. A **88**, 012710 (2013).
[22] C. Luciuk, S. Trotzky, S. Smale, Z. Yu, S. Zhang, and J. H. Thywissen, Nat. Phys. **12**, 599 (2016).
[23] M. Waseem, T. Saito, J. Yoshida, and T. Mukaiyama, Phys. Rev. A **96**, 062704 (2017).
[24] J. Yoshida, T. Saito, M. Waseem, K. Hattori, and T. Mukaiyama, Phys. Rev. Lett. **120**, 133401 (2018).
[25] M. Waseem, J. Yoshida, T. Saito, and T. Mukaiyama, Phys. Rev. A **98**, 020702(R) (2018).
[26] J. Levinsen, N. R. Cooper, and V. Gurarie, Phys. Rev. A **78**, 063616 (2008).
[27] A. K. Fedorov, V. I. Yudson, and G. V. Shlyapnikov, Phys. Rev. A **95**, 043615 (2017).
[28] M. Lu, N. Q. Burdick, and B. L. Lev, Phys. Rev. Lett. **108**, 215301 (2012).
[29] K. Aikawa, S. Baier, A. Frisch, M. Mark, C. Ravensbergen, and F. Ferlaino, Science **345**, 1484 (2014).
[30] S. S. Botelho and C. A. R. Sa de Melo, J. Low Temp. Phys. **140**, 409 (2005).
[31] T.-L. Ho and R. B. Diener, Phys. Rev. Lett. **94**, 090402 (2005).
[32] V. Gurarie, L. Radzihovsky, and A. V. Andreev, Phys. Rev. Lett. **94**, 230403 (2005).
[33] C.-H. Cheng and S.-K. Yip, Phys. Rev. Lett. **95**, 070404 (2005).
[34] M. Iskin and C. A. R. Sá de Melo, Phys. Rev. Lett. **96**, 040402 (2006).
[35] G. Cao, L. He, and P. Zhuang, Phys. Rev. A **87**, 013613 (2013).

[36] Y. Ohashi, Phys. Rev. Lett. **94**, 050403 (2005).

[37] D. Inotani, R. Watanabe, M. Sigrist, and Y. Ohashi, Phys. Rev. A **85**, 053628 (2012).

[38] D. Inotani and Y. Ohashi, Phys. Rev. A **92**, 063638 (2015).

[39] G. Cao, L. He, and X.-G. Huang, Phys. Rev. A **96**, 063618 (2017).

[40] S. M. Yoshida and M. Ueda, Phys. Rev. Lett. **115**, 135303 (2015).

[41] Z. Yu, J. H. Thywissen, and S. Zhang, Phys. Rev. Lett. **115**, 135304 (2015).

[42] M. He, S. Zhang, H. M. Chan, and Q. Zhou, Phys. Rev. Lett. **116**, 045301 (2016).

[43] S.-G. Peng, X.-J. Liu, and H. Hu, Phys. Rev. A **94**, 063651 (2016).

[44] Y.-C. Zhang and S. Zhang, Phys. Rev. A **95**, 023603 (2017).

[45] J. Yao and S. Zhang, Phys. Rev. A **97**, 043612 (2018).

[46] D. Inotani and Y. Ohashi, Phys. Rev. A **98**, 023603 (2018).

[47] S. Tan, Ann. Phys. (NY) **323**, 2952 (2008).

[48] E. Braaten and L. Platter, Phys. Rev. Lett. **100**, 205301 (2008).

[49] G. Liu and Y.-C. Zhang, Europhys. Lett. **122**, 40006 (2018).

[50] S.-J. Jiang and F. Zhou, Phys. Rev. A **97**, 063606 (2018).

[51] H. Hu, X.-J. Liu, and P. D. Drummond, Europhys. Lett. **74**, 574 (2006).

[52] R. B. Diener, R. Sensarma, and M. Randeria, Phys. Rev. A **77**, 023626 (2008).

[53] H. Hu, P. D. Drummond, and X.-J. Liu, Nat. Phys. **3**, 469 (2007).

[54] L. He, H. Lü, G. Cao, H. Hu, and X.-J. Liu, Phys. Rev. A **92**, 023620 (2015).

[55] G. Bighin and L. Salasnich, Phys. Rev. B **93**, 014519 (2016).

[56] A. A. Abrikosov, L. Gor'kov, and I. E. Dzyaloshinski, *Methods of Quantum Field Theory in Statistical Physics* (Dover, New York, 1963).

[57] In cold-atom experiments on 2D weakly interacting Bose gases with the number of atoms $N \sim 10^4$, the interaction strength g_B is typically about $(0.02\text{–}0.13)\hbar^2/m_B$. Here, the molecular gas in the BEC limit has a moderate interaction strength of $g_B \sim \hbar^2/m_B$.

[58] S. Nascimbène, N. Navon, K. Jiang, F. Chevy, and C. Salomon, Nature (London) **463**, 1057 (2010).

[59] In order to have a smoking gun proof of the nontrivial topological properties of the Fermi superfluid, it is necessary to confirm the existence of the chiral Majorana mode at the edge or the non-Abelian Majorana fermions at the vortex core.

[60] R. B. Diener and T.-L. Ho, arXiv:cond-mat/0405174.

[61] X.-J. Liu and H. Hu, Phys. Rev. A **72**, 063613 (2005).

[62] Y. Ohashi and A. Griffin, Phys. Rev. A **67**, 063612 (2003).

[63] In our numerical GPF calculations, we avoid some approximations made by Jiang and Zhou to the two-loop diagrams for obtaining a closed analytic form for the thermodynamic potential [50].

[64] U. Toniolo, B. C. Mulkerin, C. J. Vale, X.-J. Liu, and H. Hu, Phys. Rev. A **96**, 041604(R) (2017).

[65] B. C. Mulkerin, L. He, P. Dyke, C. J. Vale, X.-J. Liu, and H. Hu, Phys. Rev. A **96**, 053608 (2017).

[66] V. L. Berezinskii, Zh. Eksp. Teor. Fiz. **61**, 1144 (1971) [Sov. Phys. JETP **34**, 610 (1972)].

[67] J. M. Kosterlitz and D. J. Thouless, J. Phys. C **6**, 1181 (1973).

[68] D. R. Nelson and J. M. Kosterlitz, Phys. Rev. Lett. **39**, 1201 (1977).

[69] I. M. Khalatnikov, *An Introduction to the Theory of Superfluidity* (Perseus Books Group, Boulder, CO, 2000).

[70] N. Prokof'ev, O. Ruebenacker, and B. Svistunov, Phys. Rev. Lett. **87**, 270402 (2001).

[71] Y. Nishida, S. Moroz, and D. T. Son, Phys. Rev. Lett. **110**, 235301 (2013).